Materials Research Express

PAPER

Preclinical characterization and safety of a novel hydrogel for augmenting dural repair

RECEIVED
6 May 2015

REVISED
5 July 2015

ACCEPTED FOR PUBLICATION
21 July 2015

PUBLISHED
1 September 2015

Michael J Strong[1], **Michael A Carnahan**[2], **Keith D'Alessio**[2], **Jared D G Butlin**[2], **Mark T Butt**[3] **and Anthony L Asher**[4]

[1] Tulane University School of Medicine, New Orleans, LA, USA
[2] HyperBranch Medical Technology, Inc., Durham, NC, USA
[3] Tox Path Specialists, LCC, Frederick, MD, USA
[4] Neuroscience Institute, Carolinas Healthcare System and Carolina Neurosurgery and Spine Associates, 225 Baldwin Road, Charlotte, NC, USA

E-mail: Tony.Asher@cnsa.com

Keywords: hydrogel, polyethylene glycol, dural sealant, dural repair, CSF leakage

Supplementary material for this article is available online

Abstract

Cerebrospinal fluid (CSF) leakage is a potentially serious complication in surgical procedures involving opening of the dura mater. Although several materials have been developed to help achieve watertight dural closures, CSF leakages persist. The goal of this study was to evaluate the performance of a novel hydrogel designed to provide augmentation to standard methods of dural repair. Performance measures such as polymerization time, dimensional swelling, burst strength, and elasticity were examined in laboratory situations. Additionally, biocompatibility in an *in vivo* rat model was examined. The results demonstrate that this novel hydrogel has superior mechanical strength and tissue adherence with enhanced flexibility, reduced swelling, and quicker set time compared with existing hydrogel dural sealants approved for intra-cranial use. Furthermore, biocompatibility studies demonstrate that this compound is both non-toxic and non-immunogenic.

1. Introduction

Cerebrospinal fluid (CSF) is an essential component of the central nervous system serving numerous functions including, buoyancy, protection, chemical stability, and clearing waste [1]. The dura mater serves as the final barrier in preventing CSF leakage around the brain and spine. Oftentimes, neurosurgical interventions require opening of the dura mater. Technical challenges often preclude watertight dural closure. In fact, the reported incidence of postoperative CSF leakage ranges from 10 to 27% but can reach as high as 42% [2–11]. CSF leakage may result in several complications including meningitis, pseudomeningoceles, impaired wound healing, and subgaleal fluid collection [12]. Achieving a watertight dural closure not only reduces complications associated with CSF leakage but also reduces associated healthcare costs [13].

Currently, dural repairs are accomplished with a variety of methods including sutures, adhesives, hemostatic agents, hydrogels, and dural substitutes. The latter category includes autologous, allogenic or xenogeneic collagenic connective tissue grafts and synthetic grafts [14, 15]. These products, despite their frequent use in the clinical setting, are associated with several potential disadvantages including increased incidence of viral transmission [16], nerve compression [17–19], inadequate sealing ability [20] and direct toxicity [21, 22]. Due to the prevalence of dural defects following neurosurgical procedures and the fact that CSF leakage remains a risk despite present techniques, a new dural repair system is desirable to improve on current surgical approaches.

This study evaluated the performance of a novel hydrogel designed to provide augmentation to standard methods of dural repair. Specifically, characteristics relevant to use of such agents in biological settings, such as set time, dimensional swelling, burst strength, and elasticity, were examined. Additionally, biocompatibility, specifically neurotoxicity, was evaluated using an *in vivo* rat model. The results demonstrate that this novel

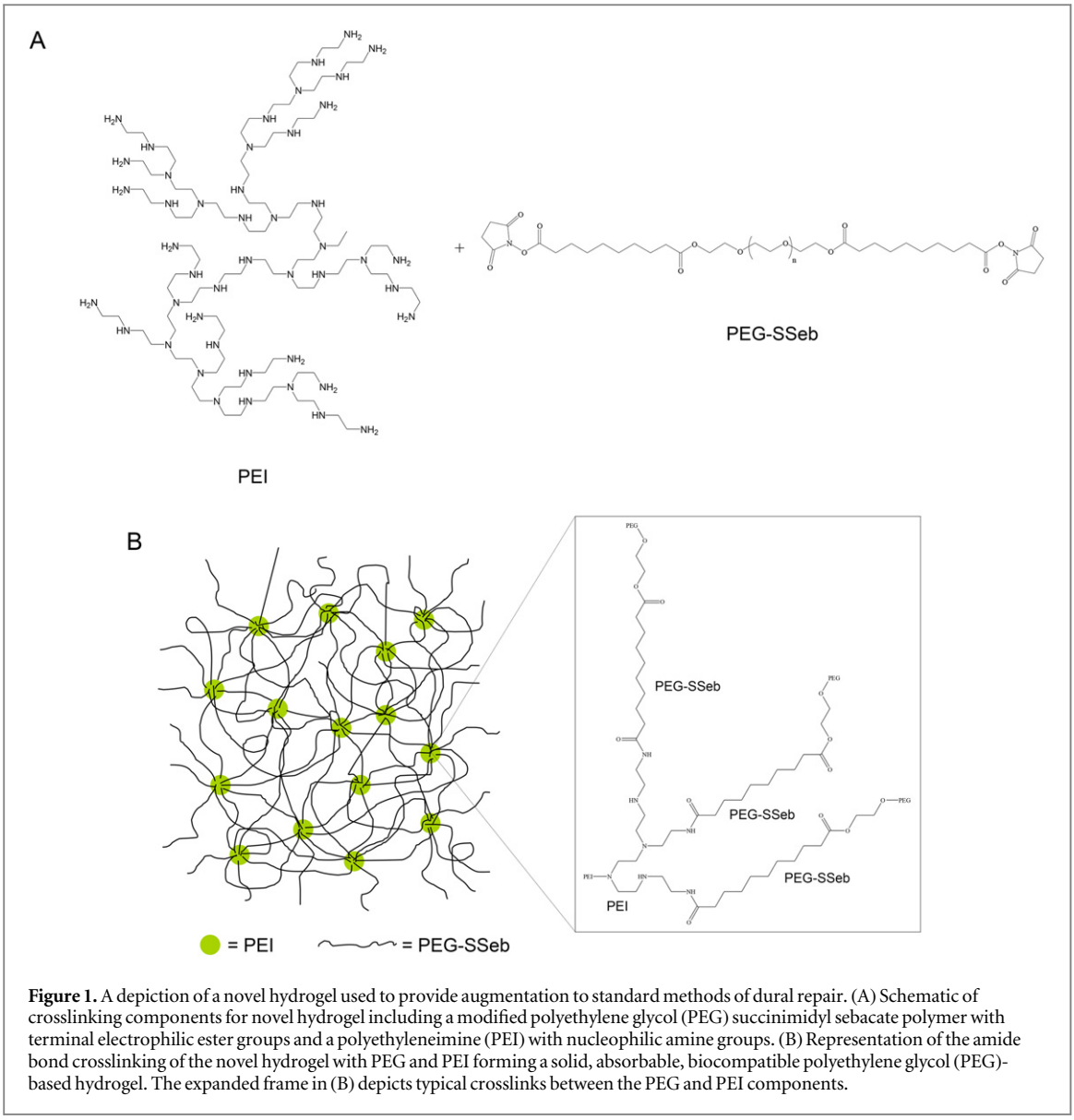

Figure 1. A depiction of a novel hydrogel used to provide augmentation to standard methods of dural repair. (A) Schematic of crosslinking components for novel hydrogel including a modified polyethylene glycol (PEG) succinimidyl sebacate polymer with terminal electrophilic ester groups and a polyethyleneimine (PEI) with nucleophilic amine groups. (B) Representation of the amide bond crosslinking of the novel hydrogel with PEG and PEI forming a solid, absorbable, biocompatible polyethylene glycol (PEG)-based hydrogel. The expanded frame in (B) depicts typical crosslinks between the PEG and PEI components.

hydrogel has superior mechanical strength and tissue adherence with enhanced flexibility, reduced swelling, and quicker set time compared with existing hydrogel dural sealants approved for intra-cranial use. Furthermore, biocompatibility studies demonstrate that this compound is both non-toxic and non-immunogenic.

2. Materials and methods

2.1. Adherus Dural Sealant

The Adherus Dural Sealant system (HyperBranch Medical Technology, Durham, NC) is a novel hydrogel sealant designed for use as an adjunct to standard methods of dural repair (e.g., sutures) to achieve watertight closure. Once reconstituted, the sealant system consists of two precursor solutions, one containing a modified polyethylene glycol (PEG) succinimidyl sebacate polymer (approximate molecular weight = 3900 Da) with two terminal electrophilic ester groups, while the other solution contains polyethyleneimine (PEI) polymer (approximate molecular weight = 2000 Da) containing approximately 17 nucleophilic amine groups (figure 1(A)). To prepare the sealant, the two precursor solutions are mixed within the supplied applicator, resulting in crosslinking (figure 1(B)) and the formation of a solid, absorbable, biocompatible PEG-based hydrogel.

2.2. DuraSeal Sealant

The DuraSeal Dural Sealant System (Integra LifeSciences, Plainsboro, NJ) is a hydrogel-based dural sealant used to augment dural closure. The DuraSeal sealant was prepared according to manufacturer's instructions and used as a comparison to the novel PEG-based hydrogel where indicated.

2.3. Set time calculation

The set time of the novel PEG-based hydrogel was determined by adding 100 μL of the reconstituted PEG solution to an inverted microcentrifuge tube (conical portion of the tube removed), containing a magnetic micro stir bar (6.35 $\times$ 3 mm, VWR, Radnor, PA) rotating at approximately 1000 rpm. Subsequently, 100 μL of the reconstituted PEI solution was added to the vial and a calibrated stopwatch was used to record the time elapsed until no stir bar rotation was observed. The reported set time for each lot is represented as an average of at least seven separate tests.

2.4. Water uptake

Both the novel PEG-based hydrogel and DuraSeal were analyzed for water uptake. The hydrogel samples were created by injecting the reconstituted solutions into a Teflon mold (9.5 $\times$ 7.8 $\times$ 2.5 mm) using a Micromedics applicator (NUS001-2). The sealant plugs were weighed immediately after formation to establish baseline measurements. Plugs were subsequently weighed after soaking for 1, 3, 7, 10, and 15 days and at least once weekly thereafter for a duration of approximately 125 days in phosphate buffered saline (PBS; pH 7.4, 37 °C). The percent gravimetric swelling at various time intervals was calculated using the following formula:

$$\%\text{Swelling} = [(\text{Mass}-\text{Initial Mass})/\text{Initial Mass}] \times 100\% \text{ where Mass} = \text{mass at any time } t.$$

Although the direct measurements of the change in dimension was not collected, the following formula was used to calculate the relative change in dimension, assuming uniform dimensional change in each axis and a gel density approximately 1.0 g cm^{-3}:

$$\left(\left[\%\text{Swelling}_t/100\% + 1\right]^{1/3} - 1\right)100\% = \%\Delta S_t$$

where $\%\text{Swelling}_t$ = percent swelling as a function of time t and $\%\Delta S_t$ = percent change in dimension (S) as a function of time t.

The reported percent swelling or percent dimensional change for each lot represents an average of at least seven separate tests.

2.5. Young's modulus

To minimize defects in the PEG-based hydrogel, the set time was extended by approximately 30–45 s by adding a small amount of phosphoric acid to the reconstituted PEI solution and mixing thoroughly. Approximately 500 μL of the PEI and PEG solutions were subsequently mixed, quickly added to a 1 cm^3 syringe and centrifuged prior to hydrogel polymerization to eliminate air bubbles. The resulting hydrogel samples were allowed to fully cure over 18–24 h at room temperature and removed from the syringe using compressed air. The hydrogel samples were then cut to a length of approximately 25 mm. Samples were glued to a test fixture using Gorilla glue (Gorilla Glue, Cincinnati, OH). Once inside the fixture, a Shimadzu AGS-J (Shimadzu Corporation, Kyoto, Japan) test machine with 20 N load cell was used to stress each sample at a crosshead speed of 10 mm min^{-1} with a chord modulus taken at 0.1 N and 0.2 N points on the stress strain curve. The reported Young's modulus is representative of an average of at least five separate tests.

2.6. Burst strength

Burst pressure testing was conducted following the established protocol: ASTM: F 2392-04 Standard Test Method for Burst Pressure Strength of Surgical Sealants [23]. Briefly, collagen casing (#320, Nippi, Tokyo, Japan) with a uniform 3 mm diameter hole, created using a skin biopsy punch, served as the tissue substrate. The novel PEG-based hydrogel was applied to the washed collagen casing, bridging the 3 mm defect with a 1 mm thick coating of hydrogel. The sealant thickness was measured using digital calipers. Samples were either tested immediately or placed in PBS (pH 7.4, 37 °C) and tested later at various time points. Burst pressure testing consisted of placing a sample into a fixture and applying pressurized water behind the collagen substrate to determine the pressure needed to rupture the hydrogel. The water pressure at which sealant failure occurred (defined as either adhesive or cohesive failure) was recorded as the burst pressure. The method of failure, adhesive or cohesive, was also noted. The reported burst pressure for each lot is representative of an average of at least five separate tests. Burst strength testing assessed over time was performed with one representative lot of material.

Table 1. Design for parenchymal implant study.

		Number of animals per necropsy interval	
Group	Treatment	1 Week	3 Months
Control	DuraSeal Dural Sealant	4	4
Test	Adherus Dural Sealant	4	4

Table 2. Design for lateral cerebral ventricle and cisterna magna extract injection study.

			Number of animals per necropsy interval	
Group	Treatment[a]	Location	Day 5	Day 15
Control LCV	0.9% Sodium chloride	LCV	3	3
Control CM	0.9% Sodium chloride	CM	3	3
Test LCV	Adherus Dural Sealant Extract	LCV	3	3
Control CM	Adherus Dural Sealant Extract	CM	3	3

[a] Twelve animals received 22 μL of the control or test material into the left lateral cerebral ventricle (LCV). The other 12 received 19 μL of the control or test material into the cisterna magna (CM).

2.7. Animals

Sixteen male albino rats approximately 9–10 months old and weighing 310– 363 g were used for the parenchymal implant studies. Twenty-four male albino rats approximately 9 weeks old and weighing 290–345 g were used for the lateral cerebral ventricle (LCV) and cisterna magna (CM) extract injection studies (Charles River Laboratories, Portage, MI). All studies were conducted at Northern Biomedical Research (Muskegon, MI) and pathology was performed at Tox Path Specialists (Walkersville, MD) in accordance with United States Food and Drug Administration Good Laboratory Practice Regulations (21CFR Part 58), the Japanese Ministry of Health, Labor, and Welfare Good Laboratory Practice Standards Ordinance 21, and the Organization for Economic Cooperation and Development Principles of Good Laboratory Practice [C (97) 186/Final].

2.8. Parenchymal implantation

Animals were randomized into two groups, control (DuraSeal Dural Sealant) and test (Adherus Dural Sealant), as shown in table 1. The control sealant used for these experiments, DuraSeal Dural Sealant, was prepared according to manufacturer's instructions. Sealants were polymerized to a depth of approximately 1 mm on a piece of Teflon and allowed to cure for 10 min. Core samples of each hydrogel were taken using an 18-gauge blunt tipped needle. The hydrogel core was then stereotactically implanted in the brain parenchyma.

For stereotactic surgery, animals were placed in an induction chamber and anesthetized with 3%–5% halothane and 1 L min^{-1} oxygen. Once anesthetized, animals were secured into a stereotaxic frame and maintained on a mixture of 1%–3% isoflurane and 1 L min^{-1} oxygen. The surgical site was prepared by standard sterile techniques and a midline cranial incision was made. The musculature was bluntly undermined and reflected to expose the skull. A craniotomy was performed 0.48 mm anterior and 4.2 mm lateral to the Bregma (figure S1). Either the test or control sealant samples were implanted in the cerebral cortex at a depth of approximately 1.4 mm below the surface of the skull using an 18 gauge blunt-tipped needle. The craniotomy was covered with dental acrylic, and the skin incision was closed with sutures. The animals recovered from anesthesia and were given intramuscular injections of butorphanol tartrate (0.05 mg kg^{-1}; Fort Dodge Animal Health, Overland Park, KS) for analgesia and a postsurgical antibiotic, ceftiofur sodium (5.0 mg kg^{-1}; GlaxoSmithKline, Brentford, England).

2.9. LCV and CM extract injection

Animals were randomized into four groups, control LCV (0.9% sodium chloride), control CM (0.9% sodium chloride), test LCV (Adherus Dural Sealant) and test CM (Adherus Dural Sealant), as shown in table 2. The hydrogel was polymerized and allowed to cure in a sterilized vessel. Once cured, the hydrogel was placed in a 0.9% sodium chloride solution (Hospira, Lake Forest, IL) at a ratio of 4 g of hydrogel per 20 mL of solution. The hydrogel was incubated at 37 °C to 39 °C for 72 h and subsequently removed to leave the extract solution. The resulting extract solution was used within 24 h. Following extract injection, the musculature and skin over the injection site was closed with sutures. All animals recovered from anesthesia and were given intramuscular

injections of butorphanol tartrate (0.05 mg kg^{-1}) for analgesia and a postsurgical antibiotic, ceftiofur sodium (5.0 mg kg^{-1}).

For stereotactic surgery, animals were anesthetized with 5% halothane and 1 L min^{-1} oxygen, placed into a stereotaxic frame, and maintained on a mixture of 1%–3% isoflurane and 1 L min^{-1} oxygen. The surgical site was prepared by standard sterile techniques and a midline cranial incision was made. The musculature was bluntly undermined and reflected to expose the skull. For the LCV injections, a craniectomy was performed, and the control or test solution was injected at a volume of 22 μL into the LCV. The craniotomy was covered with dental acrylic, and the skin incision was closed with sutures. For the CM injections, the CM was exposed using blunt dissection. The test or control solution was injected at a volume of 19 μL into the CM.

2.10. Animal neurological assessment

Clinical signs were recorded beginning three days prior to surgery and once daily post-surgically throughout the study period. Animals were monitored for signs of clinical effects, illness, and/or death. Body weights and food consumption were recorded weekly. Neurological assessments including proprioception, motor function and righting were performed at various time points throughout the study. For the parenchymal implantation studies, neurological assessments were preformed once before surgery, on day 4 and bi-weekly after surgery. For the extract injection studies, neurological assessments were preformed once before surgery and on postoperative days 1, 2, 4, and 14.

2.11. Sample collection and preparation

Parenchymal implantation studies. At the designated necropsy intervals, 1 week and 3 months, four animals from each group were anesthetized with CO_2. After the rats were anesthetized, approximately 150 μL of CSF was obtained via needle puncture into the CM. CSF samples were analyzed for changes in chemistry and protein parameters including albumin, calcium, chloride, glucose, phosphate, potassium, sodium, and total protein. Following CSF collection, the animals were perfused via the left cardiac ventricle with a heparinized 0.001% sodium nitrite saline wash followed by 10% neutral buffered formalin (NBF) fixative. Once the animals were perfused, the brain and spinal columns were removed and placed in 10% NBF.

Extract Injection studies. At the designated necropsy intervals (day 5 and 15) three animals from each group were anesthetized with CO_2. After the rats were anesthetized, approximately 150 μL of CSF was obtained via needle puncture into the CM. CSF samples were analyzed for changes in chemistry and protein parameters including albumin, calcium, chloride, glucose, phosphate, potassium, sodium, and total protein. Following CSF collection, the animals were perfused via the left cardiac ventricle with a heparinized 0.001% sodium nitrite saline wash followed by 10% NBF fixative. Once the animals were perfused, the brain and spinal columns were removed and placed in 10% NBF.

2.12. Histopathology

All tissue sections were paraffin embedded and stained with hematoxylin and eosin (H&E) and evaluated, particularly, at the implant and injection sites for tissue response. For the parenchymal implant study, if a defect in the cerebral cortex was noted during microscopic examination and was sufficiently deep enough to measure, the approximate width of the defect was recorded. For the LCV and CM extract injection groups, the brain was sectioned into eight full coronal sections. This scheme allowed for an evaluation of biocompatibility including possible local and more distant effects of the implant. The brain sections included at a minimum the following regions: neocortex (including frontal, parietal, temporal and occipital cortex and the approximate site of the implantation), paleocortex (olfactory bulbs and/or piriform cortex), basal ganglia (including caudate and putamen), limbic system (including hippocampus and cingulate gyri), thalamus/hypothalamus, midbrain regions (including substantia nigra), cerebellum, pons and medulla oblongata. For the parenchymal implant study, if a defect in the cerebral cortex was noted during microscopic examination (and was sufficiently deep to measure), the approximate width of the defect was recorded. Approximate because only the section produced for morphologic evaluation at the implant site was measured; the site was not exhaustively sectioned in order to produce a section at the true center of the implantation site. All images were taken and measurements recorded using the Olympus DP2-BSW imaging software version 2.1 (Olympus Corporation, Center Valley, PA). Transverse and oblique sections of cervical, thoracic, and lumbar spinal cord were produced and evaluated.

3. Results

3.1. Preclinical evaluation of the PEG-based hydrogel

Several factors were evaluated *in vitro* to determine the physical properties of the novel PEG-based hydrogel. These factors included polymerization time, water uptake, burst strength, and Young's modulus.

Table 3. Immediate polymerization time of novel PEG-based hydrogel.

Lot	Test 1	Test 2	Test 3	Test 4	Test 5	Test 6	Test 7
04141332	0.96	1.31	1.25	1.19	1.19	1.15	1.19
06141370	1.12	1.31	1.34	1.34	1.31	1.38	1.22
09141424	1.19	1.09	1.47	1.28	1.19	1.31	1.20

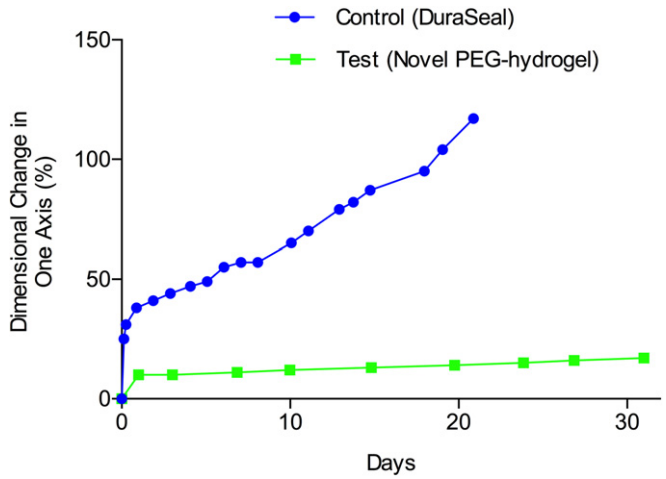

Figure 2. Dimensional change of novel PEG-based hydrogel over time. The novel hydrogel (green line) maintains its dimensional stability over time. In contrast, the control hydrogel (blue line) progressively increases in size over time.

3.1.1. Polymerization time

To test the reaction rate of the novel PEG-based hydrogel, two equal volumes of the reconstituted cross-linked components were mixed and the polymerization time was determined. The sealant reaction rate for all instances tested, including three different lots, were on average 1.2 s (range 0.96–1.47 s) after mixing (table 3). In order to assess whether the shelf life of the product affected polymerization time, precursor components of varying shelf lives were mixed in a similar fashion and all set times occurred within one second (table S1), indicating the precursor components were stable for at least 24 months.

3.1.2. Dimensional stability

Since hydrogels, when placed in a solution, absorb liquid until the cross-linked hydrogel network is fully hydrated, the amount of solution absorbed, referred to as equilibrium swelling, was determined by measuring the change in the hydrogel's mass. Since most hydrogels absorb the greatest amount of solution within the first 16–24 h, we evaluated water uptake of the novel PEG-based hydrogel plugs at 24 h and observed minimal water uptake with an average of 27% by weight (range 21–33%), when compared to the gel's initial mass (table S2). Using these observed gravimetric changes, we calculated an average 8% change in dimension along any one axis (table S3), suggesting the novel PEG-based hydrogel maintains its architecture with minimal swelling once subjected to water.

3.1.3. Dissolution and long-term dimensional stability analyses

The process of hydrolyzing ester linkages embedded within the cross-linked hydrogel structure creates a more relaxed polymer network, thus allowing more uptake of water. This hydrolytic degradation will eventually dissolve the hydrogel. To determine the amount of time before complete dissolution of the PEG-based hydrogel, water uptake studies were carried out for up to 125 days. The novel hydrogel underwent minimal dimensional changes within the first 24 h and remained relatively stable over the next 30 days (figure 2). Over the course of 90–125 days, the PEG-based hydrogel underwent complete hydrolysis of the ester linkages resulting in complete dissolution of the remaining hydrogel material with subsequent increase in swelling (figure S2). As a comparison, the DuraSeal hydrogel was also evaluated for water uptake. As shown in figure 2, DuraSeal swelled to 38% within the first 24 h and continued to swell over the next 20 days. Due to the breakdown of the DuraSeal hydrogel it was only possible to evaluate time points up to 20 days rather than 125 days for the novel PEG-based hydrogel (figure S2).

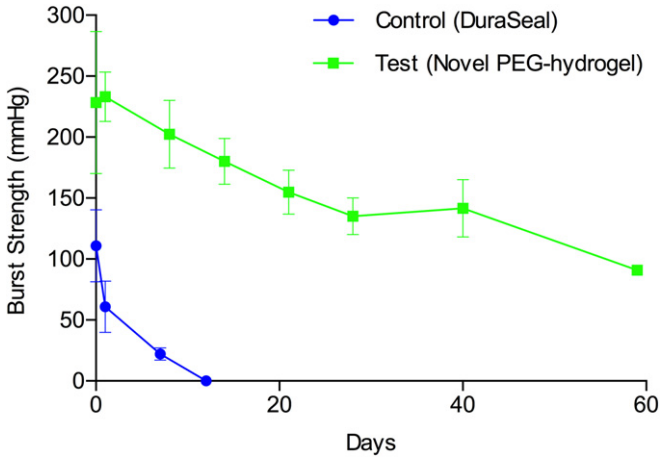

Figure 3. Average burst strength of novel PEG-based hydrogel over time. The novel hydrogel (green line) maintains supra-physiological burst strengths over time with a high initial burst strength compared to the control hydrogel (blue line).

3.1.4. Elasticity and breaking strength

The elasticity and intrinsic breaking strength of the novel PEG-based hydrogel was determined. To evaluate the elasticity of the PEG-based hydrogel, the Young's Modulus, was determined. The Young's Modulus, a measure of stiffness, was determined for the novel PEG-based hydrogel using three separate lots and ranged between 121 and 147 kPa, while the control hydrogel ranged between 6 and 11 kPa (table S4). To evaluate the intrinsic strength of the hydrogel, burst strength was determined. The novel PEG-based hydrogel was able to withstand an average burst pressure of 183 mmHg with a range of 145–254 mmHg (table S5). Similar to the set time analysis, effect of shelf life was determined with slight changes observed in burst pressure without any apparent trends.

To determine the ability of the novel PEG-based hydrogel to maintain its strength once implanted, the approximately 1 mm thick hydrogel sealant spanning the 3 mm diameter hole in the collagen casing was incubated in 37 °C PBS for several weeks before it was mounted on the test fixture. The burst strength 1 day after being submerged in PBS demonstrated an average pressure of 233 mmHg. Supra-physiological burst strengths were maintained several weeks after implantation (figure 3). In contrast, the control DuraSeal samples demonstrated an average burst strength of 82 mm Hg 1 day after submersion in PBS and could only be tested to day 7 before the integrity of the control hydrogel sample was no longer able to withstand the fluid pressure (figure 3). Of note, all of the hydrogel samples, both test and control, exhibited a cohesive failure (i.e., the hydrogel itself burst), rather than an adhesive failure (i.e., the hydrogel separated from the testing apparatus) when determining maximum burst strength pressure.

3.2. Neurological evaluation and gross visual inspection of tissues

All animals recovered from the surgical procedures and remained neurologically intact throughout the course of the study. No apparent test material related effects (e.g., body weight, food consumption, clinical pathology parameters or CSF chemistry and protein parameters) were observed between the various test groups. Furthermore, there were no test material related gross macroscopic lesions observed by visual inspection at any of the necropsy intervals.

3.3. Histopathology

3.3.1. No histological differences in test or control dural sealants on day 8 and 3 months post-parenchymal implantation

There were no histopathologic lesions observed in either the control or test groups that were directly attributed to the sealants. The changes that were observed in the brain (e.g., gliosis, hemorrhage, necrosis, macrophage infiltrates and mineralization) were observed in both groups and were likely due to the mechanical trauma of implanting the hydrogel samples in the cerebral cortex (figure 4). Within the control cerebral defect group, mineralized necrotic tissue was present, and there was evidence of minimal macrophage and neutrophil infiltrate within the surrounding meninges and cerebral cortex. Similarly, cerebral defects sealed with test sealant demonstrated minimal immune infiltrate within the cerebral cortex and surrounding meninges at the implantation site.

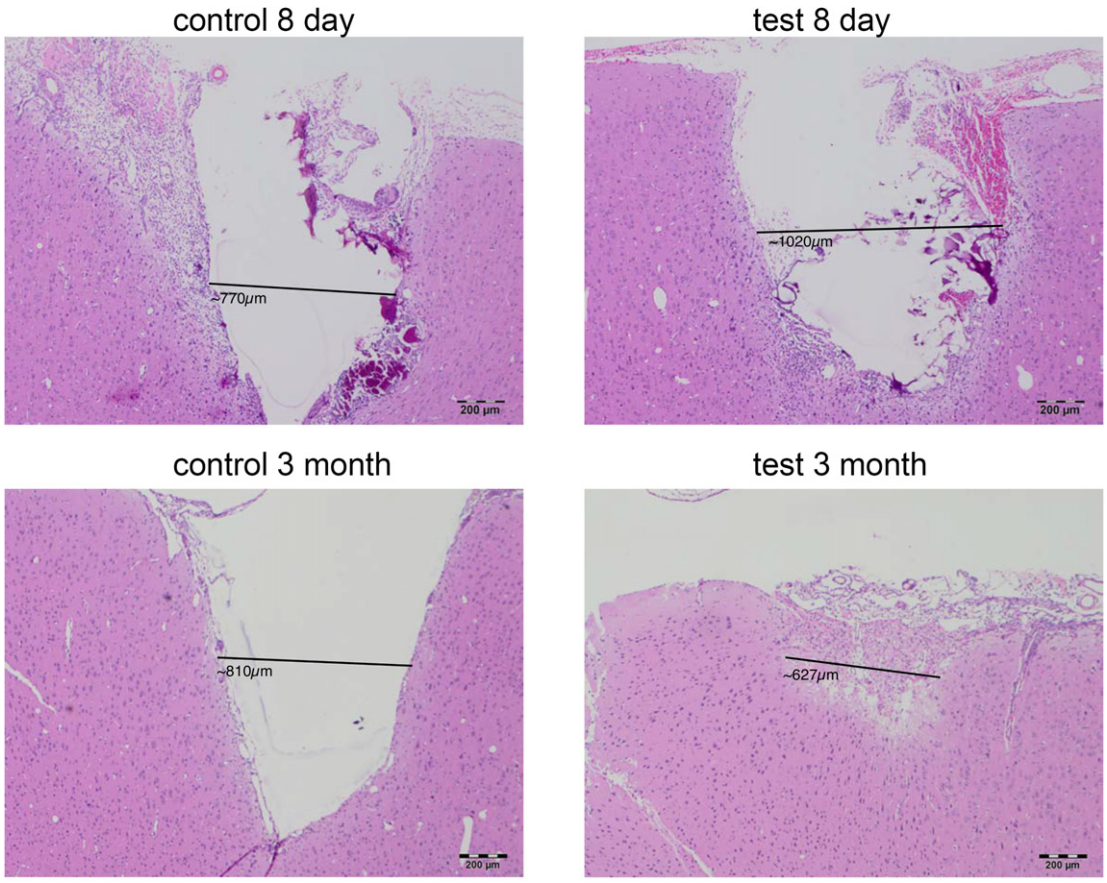

Figure 4. Representative photomicrographs of parenchymal implant H&E from control and novel PEG-based hydrogel 8 days post-procedure and 3 months post-procedure. Original magnification x4. Scale bar = 200 μm

After 3 months, no test material-related microscopic lesions were visible by histology. Consistent with the results obtained on post-operative day 8, slight gliosis at the implant site was observed. In addition, 3 month meningeal changes were similar between test groups and corresponded to results after 8 days (figure 4).

The hydrogels were visible on H&E as a basophilic material without any cellular structure. The presence of the hydrogel at the implant site on post-operative day 8 was noted in three out of the four control-treated animals (75%) and two out of the four test sealant-treated animals (50%). However, no apparent control or test hydrogel material was observed in any of the animals after 3 months (figure 4).

3.3.2. Histological evaluation of hydrogel extract and vehicle control on day 5 and 15 post-injection

Histological analysis demonstrated no significant differences between vehicle control and hydrogel LCV extract injected brains at day 5 and day 15 (figure 5). Hemorrhage in the meninges, injection site and/or in the ventricular system was observed in all animals regardless of injected material. Other microscopic changes observed 5 and 15 days post-injection included hypertrophy of endothelial cells, slight necrosis and gliosis at the injection site, and macrophage infiltrate in the meninges and injection site. One hydrogel extract-treated animal showed evidence of a few neutrophils in the brain at the injection site, but these results were thought to be consistent with mechanical manipulation rather than tissue response to the material. There were also minimal microscopic lesions in the animals that received hydrogel CM extract injection. Specifically, injection-induced hemorrhage in the meninges (brain or spinal cord) and lateral ventricles were noted in the control and test extract-treated animals in both the 5 day and 15 day groups (figure 5).

4. Discussion

Hydrogels, especially PEG-based hydrogels, have been applied in a variety of clinical and scientific settings including use as vascular sealants [24, 25], hemostatic agents [26, 27], sealants of lung air leaks [28, 29], and as tissue barriers (e.g., inhibitor of adhesions) [30–33]. Due to their unique hydrophilic crosslinking network, they are often composed of over 85% water and retain a degree of flexibility similar to human tissue. Perhaps their

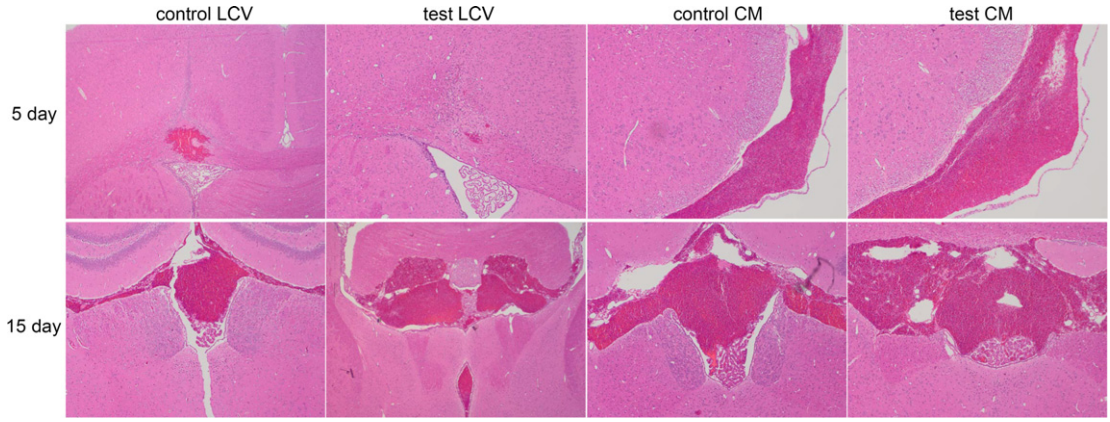

Figure 5. Representative photomicrographs of LCV extraction injection H&E from control and novel PEG-based hydrogel groups 5 days post-procedure and 15 days post-procedure. Representative photomicrographs of CM extraction injection H&E from control and novel PEG-based hydrogel groups 5 days post-procedure and 15 days post-procedure. Original magnification x4.

greatest advantage in medical applications is the ability to tune the hydrogel for a specific application or purpose. Based on these general characteristics, it was decided to optimize the development of a novel hydrogel sealant for use in neurological systems, specifically in the augmentation of standard dural repair methods.

An ideal dural hydrogel sealant must contain the following properties to be successful: (1) quick set time, (2) minimal expansion, (3) similar mechanical properties to those of the native dura mater (e.g., flexibility, strength), (4) durability, and (5) lack of toxicity or foreign body reaction. Our assessment demonstrated that the novel PEG-based hydrogel analyzed combines mechanical strength and tissue adherence with enhanced flexibility, reduced swelling, and quick set time. In addition, the composition of the hydrogel is primarily water (approximately 85% by weight) with the remaining components fully synthetic, containing no human or animal derived products, which are non-reactive and non-toxic. Finally, over time, the PEG-based hydrogel breaks down to the constituent solutions, with the majority representing PEG3400. Studies have shown that for PEGs up to 4000 Da, the major excretory route in humans is urinary clearance [34].

Since this novel PEG-based hydrogel would be in direct contact with human tissue, minimizing complications relating to microbial infections was a priority. To address this, PEI was incorporated into the hydrogel as the cross-linker. PEI is a known permeabilizer of bacteria with potent antimicrobial properties, especially when modified with hydrophobic moieties. This modified PEI has been shown to disrupt bacterial cellular membrane walls with its positive charge and degree of hydrophobicity, while remaining harmless to mammalian cells [35–37]. The hydrophobicity of the sebacic acid in combination with PEI represents a unique synergy that may confer inherent antimicrobial characteristics. *In vivo* evaluations of the antimicrobial activity of the modified PEI are ongoing.

The minimum achievable set time for a hydrogel is optimal in forming a seal at the desired location, while at the same time, reducing inadvertent run-off (which can be associated with complications arising from pooling of hydrogel in undesirable locations). In designing the novel PEG-based hydrogel, polymerization time was therefore taken into account. During our set time analysis, the novel PEG-based hydrogel sealant rapidly set (all applications) in approximately 1 s. Our analysis also included different lots of the novel PEG-based hydrogel, all of which displayed a consistent set time of approximately 1 s. These polymerization time results are considerably faster than existing PEG-based hydrogel sealants approved for cranial use (e.g., DuraSeal, which has a set time within 2 s) [12].

One explanation for this difference in observed polymerization times is differences in the physical and chemical properties between the two different hydrogel crosslinking components. A PEG-based hydrogel is formed by the reaction of two relatively small crosslinking polymers. The large number of reactive sites and the small molecular weight of the cross-linkers may enhance cross-linking efficiency by maximizing the reactive groups available for crosslinking in any particular environment, while minimizing steric constraints. For example, the novel PEG-based hydrogel sealant system is composed of a PEI polymer (approximate molecular weight = 2000 Da) with roughly 17 primary amines and a modified PEG succinimidyl sebacate polymer (approximate molecular weight = 3900 Da) with two activated esters. In contrast, DuraSeal is composed of trilysine polymer (approximate molecular weight = 402 Da) with only four primary amines and PEG succinimidyl glutarate polymer (approximate molecular weight = 20 000 Da) with four activated esters.

One disadvantage of hydrogels in neurological systems is their propensity to expand *in vivo*, as swelling can result in nerve compression [17–19]. Therefore, vital to the success of a dural sealant is the ability to minimize

water uptake and subsequent swelling within the dural space to reduce mass effect and other neurological complications. In this study, the volume expansion of the PEG-based hydrogel was minimal relative to other PEG-based hydrogels. Several hypotheses have been postulated to help explain the limited volumetric expansion of the novel PEG-based hydrogel. For instance, the ratio of PEG-SSeb to PEI is controlled in the novel PEG-based hydrogel to provide a near 1:1 ratio of primary amines on PEI with activated esters on the PEG. This ratio, therefore, creates a dense cross-linked network where each PEI polymer may be cross-linked with up to 17 different PEG polymers through ester bonds as demonstrated in figure 1. Furthermore, the novel PEG-based hydrogel is able to retain this dense cross-linked structure for at least three to four weeks by integrating ester linkages into the network that are less hydrolytically labile. It is thought that the hydrophobic properties of the sebacic acid used to introduce the ester linkages may help limit swelling. The chemical design that allows for minimal swelling therefore also prevents susceptibility to hydrolysis, allowing the PEG-based hydrogel to maintain its structural integrity throughout the healing process. These ester linkages are eventually hydrolyzed and the sealant is typically no longer visible after approximately 90 days.

A material that is both flexible and intrinsically strong is an ideal candidate for dural repair procedures. The material has to be flexible enough to ensure that stress concentrations do not occur in the native tissue being repaired, which may result in premature failure of the repaired dura. To minimize stresses between tissues and sealants, it is generally accepted that it is best to use materials with similar physical properties as tissue [38]. Although the novel PEG-based hydrogel sealant is not as stiff as native dura [39], it best matches the elastic modulus of the dura when compared to other commercially available sealants. At the same time, the material has to be strong enough to withstand the intracranial pressure giving time for the dura to heal. This dichotomy requires a fine balance of crosslinking within the hydrogel. The strength of the hydrogel is dictated by the degree of crosslinking with more crosslinking leading to a stronger hydrogel [40, 41]. However, with increased crosslinking there is less elasticity [42].

In general, physiological CSF pressure averages approximately 10 mmHg with pressure spikes generated during coughs or Valsalva maneuvers reaching as high as 45 mmHg [43, 44]. The initial burst strength and elasticity tests further support the concept of this novel PEG-based hydrogel forming a strong, well-adhered watertight barrier. During the first week following implantation, the hydrogel provides a watertight barrier that can easily withstand physiological pressures. In fact, this stable strength of the novel PEG-based hydrogel at supra-physiological levels is maintained for weeks after application, as demonstrated by our *in vitro* and *in vivo* burst strength studies.

The rat model demonstrated that the novel PEG-based hydrogel was well tolerated with no neurotoxicity nor evidence of a toxic leachable component. Minimal immune infiltrate was observed in both test groups in the implantation and extraction injection studies and were likely due to the mechanical trauma of the surgical procedure. This observation is consistent with other implantation studies, which report similar microscopic changes secondary to mechanical trauma [45–48]. Further, the absence of any difference in immune infiltrate between the test groups at 8 days and 3 months is consistent with findings from Baker *et al* in which they sprayed the same novel PEG-based hydrogel in burr holes of rats and evaluated the subsequent acute and chronic immune infiltrate response [49].

A study conducted by Bjugstad *et al* demonstrated that the inflammatory response to PEG-based hydrogels depended on the biodegradable properties of the hydrogel. Hydrogels that persisted longer elicited a greater immune response than hydrogels with a faster degradation rate [50]. Although some hydrogels may prompt an immune response over time, we did not observe this trend for the novel PEG-based hydrogel tested here, which has a slower degradation characteristic than other hydrogels. Furthermore, the immune response present in our testing was limited and more consistent with mechanical manipulation of the tissue, as stated previously.

The limited inflammatory response of hydrogels is a vast improvement over other materials used as dural sealants. In comparison, fibrin glue has been reported to invoke a foreign body reaction [51] and fibrin glue containing tranexamic acid has been shown to cause epileptic seizures in rats [22]. BioGlue, used off-label as a dural sealant, contains glutaraldehyde, which can leach from the glue causing neurotoxicity [20, 21]. Finally, although not classified as a dural sealant, gelatin sponges and oxidized cellulose polymers, often used as hemostatic agents, are associated with a significant inflammatory reaction that can be mistaken for an abscess or recurrent tumor [52, 53].

5. Conclusion

In summary, next-generation hydrogels, as in the novel PEG-based hydrogel tested in this study, can serve as more optimal adjuvants to dural repair. Since the hydrogel consists of more than 85% water once polymerized and implanted, this material possesses physical properties comparable to the native tissue. In addition, the formulation of the novel PEG-based hydrogel allows for such rapid self-polymerization that a watertight barrier

is formed within 1 s. This barrier is not only flexible but can withstand considerable supra-physiological CSF pressures. Pharmacokinetically, due to the ester linkages within the hydrogel network, this biomaterial will ultimately be hydrolyzed, leading to complete reabsorption and clearance without eliciting a foreign body response. These studies suggest superior mechanical and physiological characteristics compared with other methods of dural closure augmentation, and support the examination of this agent in more advanced biological systems, including large animal and human studies.

Acknowledgment

This work was funded by HyperBranch Medical Technology.

Conflicts of Interest

Michael Carnahan and Keith D'Alessio are currently employed by HyperBranch Medical Technology. HyperBranch Medical Technology provided funds, resources and equipment to conduct these analyses. Anthony Asher is a consultant to HyperBranch Medical Technology.

References

[1] Di Terlizzi R and Platt S 2006 The function, composition and analysis of cerebrospinal fluid in companion animals: I. Function and composition *Veterinary J.* **172** 422–31
[2] Cristante L, Westphal M and Herrmann H D 1994 Cranio-cervical decompression for Chiari I malformation. A retrospective evaluation of functional outcome with particular attention to the motor deficits *Acta Neurochir* (*Wien*) **130** 94–100
[3] Gnanalingham K K, Lafuente J, Thompson D, Harkness W and Hayward R 2003 MRI study of the natural history and risk factors for pseudomeningocoele formation following postfossa surgery in children *Br. J. Neurosurg.* **17** 530–6
[4] Gnanalingham K K, Lafuente J, Thompson D, Harkness W and Hayward R 2002 Surgical procedures for posterior fossa tumors in children: does craniotomy lead to fewer complications than craniectomy? *J. Neurosurg.* **97** 821–6
[5] Sarma S, Sekhar L N and Schessel D A 2002 Nonvestibular Schwannomas of the brain: a 7-year experience *Neurosurgery* **50** 437–48
[6] Vanaclocha V and Saiz-Sapena N 1997 Duraplasty with freeze-dried cadaveric dura versus occipital pericranium for Chiari type I malformation: comparative study *Acta Neurochir.* **139** 112–9
[7] Magliulo G, Sepe C, Varacalli S and Fusconi M 1998 Cerebrospinal fluid leak management following cerebellopontine angle surgery *J. Otolaryngol.* **27** 258–62
[8] Brennan J W, Rowed D W, Nedzelski J M and Chen J M 2001 Cerebrospinal fluid leak after acoustic neuroma surgery: influence of tumor size and surgical approach on incidence and response to treatment *J. Neurosurg.* **94** 217–23
[9] Selesnick S H, Liu J C, Jen A and Newman J 2004 The Incidence of Cerebrospinal fluid leak after vestibular schwannoma surgery *Otol. Neurotol.* **25** 387–93
[10] Yoshimoto T, Sawamura Y, Houkin K and Abe H 1997 Effectiveness of fibrin glue for preventing postoperative extradural fluid leakage *Neurologia Med.-Chirurgica* **37** 886–90
[11] Hoffman R A 1994 Cerebrospinal fluid leak following acoustic neuroma removal *Laryngoscope* **104** 40–58
[12] Cosgrove G R *et al* 2007 Safety and efficacy of a novel polyethylene glycol hydrogel sealant for watertight dural repair *J. Neurosurg.* **106** 52–8
[13] Grotenhuis J A 2005 Costs of postoperative cerebrospinal fluid leakage: 1-year, retrospective analysis of 412 consecutive nontrauma cases *Surg. Neurol.* **64** 490–3
[14] Pařízek J *et al* 1997 Detailed evaluation of 2959 allogeneic and xenogeneic dense connective tissue grafts (fascia lata, pericardium, and dura mater) used in the course of 20 years for duraplasty in neurosurgery *Acta Neurochir* **139** 827–38
[15] Yu F, Wu F, Zhou R, Guo L, Zhang J and Tao D 2013 Current developments in dural repair: a focused review on new methods and materials *Frontiers Biosci.* (*Landmark Ed.*) **18** 1335–43
[16] Dufrane D, Cornu O, Delloye C and Schneider Y J 2002 Physical and chemical processing for a human dura mater substitute *Biomaterials* **23** 2979–88
[17] Thavarajah D, De Lacy P, Hussain R and Redfern R M 2010 Postoperative cervical cord compression induced by hydrogel (DuraSeal): a possible complication *Spine* **35** E25–6
[18] Lee S-H, Park C-W, Lee S-G and Kim W-K 2013 Postoperative cervical cord compression induced by hydrogel dural sealant (DuraSeal®) *Korean J. Spine* **10** 44–6
[19] Blackburn S and Smyth M D 2007 Hydrogel-induced cervicomedullary compression after posterior fossa decompression for Chiari malformation *J. Neurosurg.: Pediatrics* **106** 302–4
[20] Epstein N E 2010 Dural repair with four spinal sealants: focused review of the manufacturers' inserts and the current literature *Spine J.* **10** 1065–8
[21] Fürst W and Banerjee A 2005 Release of glutaraldehyde from an albumin-glutaraldehyde tissue adhesive causes significant *in vitro* and *in vivo* toxicity *Ann. Thoracic Surg.* **79** 1522–8
[22] Schlag M G, Hopf R and Redl H 2000 Convulsive seizures following subdural application of fibrin sealant containing tranexamic acid in a rat model *Neurosurgery* **47** 1463–7
[23] ASTM International 2010 *F2392-04(2010) A, Standard Test Method for Burst Strength of Surgical Sealants* (West Conshohocken, PA: ASTM International) (wwwastmorg)
[24] Wallace D G *et al* 2001 A tissue sealant based on reactive multifunctional polyethylene glycol *J. Biomed. Mater. Res.* **58** 545–55
[25] Dumanian G A *et al* 1995 A new photopolymerizable blood vessel glue that seals human vessel anastomoses without augmenting thrombogenicity *Plast. Reconstr. Surg.* **95** 901–7
[26] Ramakumar S *et al* 2002 Local hemostasis during laparoscopic partial nephrectomy using biodegradable hydrogels: initial porcine results *J. Endourol.* **16** 489–94
[27] White J K, Titus J S, Tanabe H, Aretz H T and Torchiana D F 2000 The use of a novel tissue sealant as a hemostatic adjunct in cardiac surgery *Heart Surg. Forum* **3** 56–61

[28] Kobayashi H, Sekine T, Nakamura T and Shimizu Y 2001 *In vivo* evaluation of a new sealant material on a rat lung air leak model *J. Biomed. Mater. Res.* **58** 658–65
[29] Otani Y, Tabata Y and Ikada Y 1999 Sealing effect of rapidly curable gelatin-poly (l-glutamic acid) hydrogel glue on lung air leak *Ann. Thoracic Surg.* **67** 922–6
[30] Johns D A, Ferland R and Dunn R 2003 Initial feasibility study of a sprayable hydrogel adhesion barrier system in patients undergoing laparoscopic ovarian surgery *J. Am. Assoc. Gynecol. Laparoscopists* **10** 334–8
[31] Wechsler S, Fehr D, Molenberg A, Raeber G, Schense J C and Weber F E 2008 A novel, tissue occlusive poly(ethylene glycol) hydrogel material *J. Biomed. Mater. Res.* A **85A** 285–92
[32] Ferland R, Mulani D and Campbell P K 2001 Evaluation of a sprayable polyethylene glycol adhesion barrier in a porcine efficacy model *Hum. Reprod.* **16** 2718–23
[33] Preul M C, Bichard W D, Muench T R and Spetzler R F 2003 Toward optimal tissue sealants for neurosurgery: use of a novel hydrogel sealant in a canine durotomy repair model *Neurosurgery* **53** 1189–99
[34] Webster R *et al* 2007 PEGylated proteins: evaluation of their safety in the absence of definitive metabolism studies *Drug Metabolism Disposition* **35** 9–16
[35] Helander I M, Alakomi H-L, Latva-Kala K and Koski P 1997 Polyethyleneimine is an effective permeabilizer of gram-negative bacteria *Microbiology* **143** 3193–9
[36] Haldar J, An D, Álvarez de Cienfuegos L, Chen J and Klibanov A M 2006 Polymeric coatings that inactivate both influenza virus and pathogenic bacteria *Proc. Natl Acad. Sci. USA* **103** 17667–71
[37] Lin J, Qiu S, Lewis K and Klibanov A M 2003 Mechanism of bactericidal and fungicidal activities of textiles covalently modified with alkylated polyethylenimine *Biotechnol. Bioeng.* **83** 168–72
[38] Nguyen K T and West J L 2002 Photopolymerizable hydrogels for tissue engineering applications *Biomaterials* **23** 4307–14
[39] Runza M, Pietrabissa R, Mantero S, Albani A, Quaglini V and Contro R 1999 Lumbar dura mater biomechanics: experimental characterization and scanning electron microscopy observations *Anesth. Analg.* **88** 1317–21
[40] Hoffman A S 2002 Hydrogels for biomedical applications *Adv. Drug Deliv. Rev.* **54** 3–12
[41] Lin C-C and Metters A T 2006 Hydrogels in controlled release formulations: network design and mathematical modeling *Adv. Drug Deliv. Rev.* **58** 1379–408
[42] Zhu J and Marchant R E 2011 Design properties of hydrogel tissue-engineering scaffolds *Expert Rev. Med. Devices* **8** 607–26
[43] Neville L and Egan R A 2005 Frequency and amplitude of elevation of cerebrospinal fluid resting pressure by the Valsalva maneuver *Can. J. Ophthalmol. (Journal Canadien d'Ophtalmologie)* **40** 775–7
[44] Bono F, Giliberto C, Lavano A and Quattrone A 2005 Posture-related cough headache and orthostatic drop in lumbar CSF pressure *J. Neurol.* **252** 237–8
[45] Stensaas S S and Stensaas L J 1978 Histopathological evaluation of materials implanted in the cerebral cortex *Acta Neuropathol.* **41** 145–55
[46] Stensaas S S and Stensaas L J 1976 The reaction of the cerebral cortex to chronically implanted plastic needles *Acta Neuropathol.* **35** 187–203
[47] Winn S R, Aebischer P and Galletti P M 1989 Brain tissue reaction to permselective polymer capsules *J. Biomed. Mater. Res.* **23** 31–44
[48] Kim Y-T, Hitchcock R W, Bridge M J and Tresco P A 2004 Chronic response of adult rat brain tissue to implants anchored to the skull *Biomaterials* **25** 2229–37
[49] Bakar B *et al* 2013 Evaluation of the neurotoxicity of the polyethylene glycol hydrogel dural sealant *Turk. Neurosurg.* **23** 16–24
[50] Bjugstad K B, Lampe K, Kern D S and Mahoney M 2010 Biocompatibility of poly(ethylene glycol)-based hydrogels in the brain: an analysis of the glial response across space and time *J. Biomed. Mater. Res.* A **95A** 79–91
[51] Sanal M, Dogruyol H, Gurpinar A and Yerci O 1992 Does fibrin glue cause foreign body reactions? *Eur. J. Pediatric Surg.: Off. J. Austrian Assoc. Pediatric Surg. [et al] = Z. Kinderchirurgie* **2** 285–6
[52] Buckley S C and Broome J C 1995 A foreign body reaction to surgical mimicking an abscess or tumour recurrence *Br. J. Neurosurg.* **9** 561
[53] Kothbauer K F, Jallo G I, Siffert J, Jimenez E, Allen J C and Epstein F J 2001 Foreign body reaction to hemostatic materials mimicking recurrent brain tumor *J. Neurosurg.* **95** 503–6